Membrane Lysis by the Antibacterial Peptides Cecropins B1 and B3: A Spin-Label Electron Spin Resonance Study on Phospholipid Bilayers

ARTICLE *in* BIOPHYSICAL JOURNAL · JANUARY 2000

Impact Factor: 3.97 · DOI: 10.1016/S0006-3495(99)77142-0 · Source: PubMed

4 AUTHORS, INCLUDING:

Sunney I Chan
Academia Sinica
388 PUBLICATIONS **11,302** CITATIONS

SEE PROFILE

Membrane Lysis by the Antibacterial Peptides Cecropins B1 and B3: A Spin-Label Electron Spin Resonance Study on Phospholipid Bilayers

Shao-Ching Hung,* Wei Wang,# Sunney I. Chan,* and Hueih Min Chen#

From the #Department of Biochemistry, Hong Kong University of Science and Technology, Clear Water Bay, Kowloon, Hong Kong and the *Division of Chemistry and Chemical Engineering, California Institute of Technology, Pasadena, California 91125, USA

ABSTRACT Custom antibacterial peptides, cecropins B1 (CB1) and B3 (CB3), were synthesized. These peptides have particular sequence characteristics, with CB1 having two amphipathic α-helical segments and CB3 having two hydrophobic α-helical segments. These differences were exploited for a study of their efficacy in breaking up liposomes, which had different combinations of phosphatidic acid (PA) and phosphatidylcholine (PC), and a study of their lipid binding ability. Binding and nonbinding lysis actions of CB1 and CB3 on liposomes were examined further by electron spin resonance (ESR). The spin-labeled lipids 5′SL-PC, 7′SL-PC, 10′SL-PC, 12′SL-PC, and 16′SL-PC were used as probes. The ESR spectra revealed larger outer hyperfine splittings ($2A_{max}$) for CB1 when the interactions of CB1 and CB3 with liposomes were compared. These observations indicate a larger restriction of the motion of the spin-labeled chains in the presence of CB1. Plots of the effective order parameter at the various probe positions (chain flexibility gradient) versus the peptide–lipid ratio further suggested that the lysis action of CB1 is related to its capacity to bind to the lipid bilayers. In contrast, there is no evidence of binding for CB3. To augment these findings, four spin-labeled peptides, C8SL-CB1, C32SL-CB1, C5SL-CB3, and C30SL-CB3, were also examined for their binding to and their state of aggregation within the lipid bilayers. Association isotherms of the peptides were measured for liposomes containing two molar fractions of PA (0.25 and 0.75). The membrane binding of the CB1 peptides exhibited a cooperative behavior, whereas the association isotherm of CB3 revealed binding to the lipid only for $\beta = 0.75$ liposomes. To further identify the location of CB1 in the lipid bilayers, measurements of the collision rate with chromium oxalate in solution were conducted. Results from ESR power saturation measurements suggested that the NH_2-terminal α-helix of CB1 is located on the surface of the lipid bilayers, whereas the COOH-terminal α-helix of CB1 is embedded below the surface of the lipid bilayers. These conclusions were further supported by the observed relationship between the partition distribution of peptides bound to liposomes at different PA/PC ratios and the amounts of free peptides. Based on the above observations, possible mechanisms of the bilayer lysis induced by CB1 and CB3 on liposomes of different composition are discussed.

INTRODUCTION

Cecropins were originally isolated from immune hemolymph of the moth *Hyalophora cecropia* (Hultmark et al., 1980; Steiner et al., 1981) and later from other insects (Boman, 1991; Hultmark, 1993) as agents that kill bacteria. These antibacterial peptides may also exist in the broader spectrum of the animal kingdom because a mammalian cecropin P1 has been isolated from porcine small intestine (Lee et al., 1989). In addition to their action on bacteria, cecropins and other antibacterial peptides, such as magainins and their analogs, were found to be able to lyse hematopoietic and solid tumor cells with few toxic effects on normal blood lymphocytes (Jaynes et al., 1989; Cruciani et al., 1991). These short proteins have, therefore, been referred to as aBaM.

The sequences of cecropin peptides, which range from 31 to 39 amino acids, are highly conserved with a high proportion of the basic amino acids. The helical conformation of cecropin A in hexafluoro-2-propanol solution was originally confirmed by circular dichroism spectroscopy (Steiner, 1982). Subsequently, its two-dimensional nuclear magnetic resonance structure was established (Holak et al., 1988): the peptide folds into two lobes with an NH_2-terminal amphipathic helix and a COOH-terminal hydrophobic helix joined by an Ala-Gly-Pro segment. The maintenance of the α-helical structure of cecropins may be one of the key factors that enable them to disrupt cell membranes. However, the details of the correlation between the extent and stability of the secondary structure of the peptides and their cell-killing ability remain unknown. Another possible key factor that may influence membrane lysis is the association of these peptides with lipid bilayers. This binding effect was confirmed by evidence of voltage-dependent channel formation by cecropins (Christensen et al., 1988), magainins (Agawa et al., 1991), and defensins (Kagan et al., 1990; Cociancich et al., 1993) in lipid bilayers. That membrane lysis may be through pore formation was further suggested by the observation that encapsulated ions or other solutes could be selectively released from lipid bilayer vesicles

Received for publication 11 March 1999 and in final form 24 August 1999.

Address reprint requests to Dr. H. M. Chen, Department of Biochemistry, Hong Kong University of Science and Technology, Clear Water Bay, Kowloon, Hong Kong. Tel.: +852-2358-7294; Fax: +852-2358-1552; E-mail: bchmc@ust.hk.

Abbreviations used: aBaM, antibacterial/antimalignant peptides; CB, cecropin B; CB1, cecropin B1; CB3, cecropin B3; Crox, potassium chromium III oxalate trihydrate; DOXYL, nitroxide spin; HPLC, high performance liquid chromatograph; MTSSL, (1-oxyl-2,2,5,5-tetramethylphyrroline-3-methyl) methanethiosulfonate; PA, phosphatidic acid; PC, phosphatidylcholine; β, fraction of PA (PA/(PA + PC)).

0006-3495/99/12/3120/14 $2.00

upon the addition of the peptides (Saberwal and Nagaraj, 1994; Boman, 1995; Matsuzaki et al., 1997).

However, the mechanisms by which aBaM peptides cause cell death are not fully understood yet. It is generally believed that the peptides associate with the membrane to form structural domains, which either aggregate and form pores within the membrane, or cover the membrane with a detergent-like carpet of molecules, which then destabilizes the packing of the lipids in the membrane (Pouny et al., 1992; Merrifield et al., 1994; Gazit et al., 1995). The latter mechanism was suggested by the high peptide stoichiometry required for membrane lysis (Steiner et al., 1988; Pouny et al., 1992). In contrast, only the initial or final stages of membrane lysis have been reported to date. The detailed time course of membrane permeabilization induced by aBaM peptides remains elusive. Regardless of the killing pathway, however, it appears that the initial association of the peptides with the membranes followed by the self-association of the peptides near the negatively charged lipid domains may be the key determinants governing the specificity and effectiveness of the peptides. Extensive studies on the role of electrostatic interactions in the binding of cationic peptides to anionic lipid bilayers by theoretical and experimental approaches have been conducted by the Honig and McLaughlin groups (Kim et al., 1991; Ben-Tal et al., 1997a,b). White and coworkers have also demonstrated the significance of the anionic content of the membrane on the ability of cationic peptides to induce membrane lysis (Wimley et al., 1994; Hristova et al., 1997).

In earlier work, we have studied the effect of aBaM peptides on cell membranes by examining the actions of CB and its analogs, CB1, CB2, and CB3, on liposomes, bacteria, and cancer cells (Chen et al., 1997). The results revealed that lytic peptides, designed to have extra cationic residues, were less effective at breaking up liposomes and killing bacteria, but more effective in lysing cancer cells. CB3 showed no effect on either bacteria or cancer cells. In addition to the experiments on living cells, we also investigated the role of membrane composition and the physical characteristics of the cecropin peptides in liposome lysis (Wang et al., 1998). The actions of CB, CB1, and CB3 on membranes consisting of varying ratios of PA and PC were examined. The results indicated that the higher binding affinity of CB and CB1 to the polar headgroups of the lipids was not a precondition for the peptides to be more effective at lysing lipid bilayers, especially with liposomes of higher PA contents. Moreover, CB3 showed no binding, or only weak binding, to liposomes, but its ability to cause dye-leakage was higher than CB and CB1, if the PA content in the liposomes was high. Intrinsic and extrinsic stopped-flow fluorescence measurements further revealed that CB and CB1 exhibited different kinetic steps in liposomal breakage from CB3 (Wang et al., 1998). Thus, the lytic pathways used by CB or CB1 on living cells and liposomes are different from those used by CB3.

In this report, we augment our earlier observations by examining the interactions of the cecropin peptides with lipid bilayers by means of electron spin resonance (ESR) (Marsh and Watts, 1981; Tanaka and Freed, 1985; Ge and Freed, 1993). Spin-labeled lipids have been used by Marsh and coworkers to investigate the insertion of diphtheria toxin into lipid bilayers (Montich et al., 1995) as well as the interaction of melittin peptides with neutral and anionic phospholipid bilayers (Kleinschmidt et al., 1997). They reported that the binding of melittin to the lipid bilayers initially caused a restriction of lipid acyl chain motions. Feix and coworkers have also used the ESR method to study the binding and the state of aggregation of spin-labeled cecropin AD in hexafluoro-2-propanol solution (Mchaourab et al., 1993) and within phospholipid bilayers, and have proposed a scheme for the interaction between cecropin AD and membranes (Mchaourab et al., 1994). However, only one molecule was spin-labeled (lipid or peptide) and only one kind of peptide was used for these studies. In the present study, both spin-labeled lipids and spin-labeled peptides are used in the ESR experiments. We focus on the effects of CB1, which is characterized by two amphipathic α-helices, and CB3, which has two hydrophobic α-helices, on liposomes of different compositions. The basis for the binding and nonbinding modes of membrane lysis by these peptides on liposomes of different compositions will be elucidated. Since the membrane permeabilization induced by CB and CB1 are similar (Wang et al., 1998), these findings should bear on the action of CB.

EXPERIMENTAL PROCEDURES

Materials

PC and PA, of 95% and 98% purity, respectively, were purchased from Sigma Chemical Co. (St. Louis, MO). The product PC is composed by about 53% unsaturated and 47% saturated PC. Over 95% of PC have the chain lengths of 16 and 18. DOXYL fatty acid labels was obtained from Avanti Polar Lipids Inc. (Alabaster, AL). Spin-labeled PCs with the DOXYL at various positions down the hydrophobic chain of PC (5′SL-PC, 7′SL-PC, 10′SL-PC, 12′SL-PC, and 16′SL-PC) were then prepared. The spin-labeled PCs allow the membrane bilayers to be probed at various depths (see Fig. 1). They were synthesized by condensation of 1-palmitoyl-2-hydroxy-*sn*-glycerol-3-phosphocholine and the various DOXYL-labeled fatty acids. Purity was typically greater than 99% after HPLC purification (Yin and Hyde, 1989; Dejongh et al., 1990). To spin label the peptides, MTSSL was purchased from Reanal Chemical Co. (Hungary). MTSSL reacts very effectively with protein thiol groups to form a disulfide bond, generating a nitroxide-labeled side chain (Millhauser, 1992; Oh et al., 1996). Crox was purchased from Aldrich Chemical Co. (Milwaukee, WI). Sodium chloride was certified to be Fisher grade. Monobasic, monohydrate sodium phosphate and dibasic, anhydrous sodium phophate were purchased from Sigma. Only deionized and distilled water was used in the experiments.

Preparation of liposomes

Liposomes, with or without spin-labeled lipids, 4% (w/w), of different compositions (β = PA/(PA + PC)) were prepared in phosphate-buffered saline (PBS) (10 mM sodium phosphate and 100 mM sodium chloride at pH 7.4) using the sonication method. A 20-mg mixture of PA and PC (4% spin-labeled PC), with β varying from 0 to 1, was dissolved in 1 ml chloroform. After gently shaking to dissolve the solid, the chloroform was

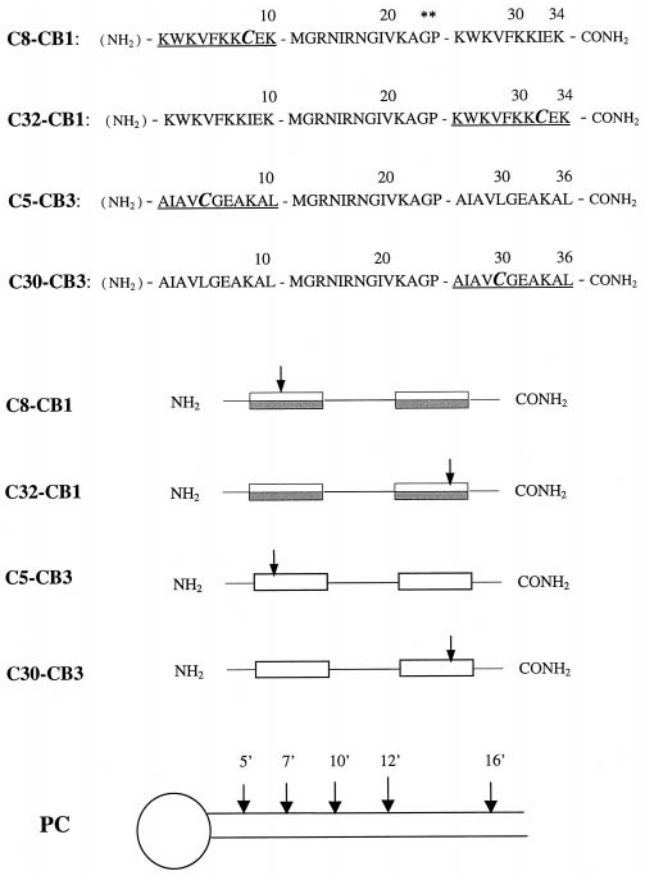

FIGURE 1 Amino acid sequences and cartoon structures of the spin-labeled CB1 and CB3 derivatives and spin-labeled lipids. In C8SL-CB1 and C32SL-CB1, the underlined segments indicate the NH_2-terminal and COOH-terminal amphipathic helices of CB1 with a spin-labeled Cys (***C***), respectively. The hinge between the two helices is at Gly^{23} and Pro^{24} (*). Both sequences of the spin-labeled CB1 derivatives are identical to those of CB1 (Wang et al., 1998)), except that Ile^{8} and Ala^{32} are replaced by Cys (***C***) for C8SL-CB1 and C32SL-CB1, respectively. Similarly, both sequences of the spin-labeled CB3 derivatives are identical to that of CB3, except that Leu^{5} and Leu^{30} are replaced by Cys for C5SL-CB3 and C30SL-CB3, respectively. The structures of the various peptides are indicated by cartoons: amphipathic and hydrophobic helices are represented by partly shaded and open rectangles, respectively. The location of the spin-labeled MTSSL in both of the peptides is shown by an arrow. The DOXYL spin-labeled PC at various positions of the lipid chain is also shown. For each spin-labeled PC, only the 2′-chain is labeled at one of the positions indicated by the arrow ($n' = 5, 7, 10, 12, 16$).

removed by an argon stream. The lipid was then rehydrated and dispersed into 2 ml PBS at pH 7.4. The milky solution was sonicated (model G112 SPIT, Laboratory Supplies Co., Hicksville, NY) at 300 W for at least 4 h until the solution became clear. This procedure typically produces sonicated single-bilayer vesicles of the order of 300 Å in diameter. Lipid concentration was determined by a phospholipid reagent (Wako Pure Chemical Industries, Tokyo, Japan) using the Barlett assay (Barlett, 1959). The results were expressed in terms of the concentration of phosphorus. Stock solutions of spin labeled lipids (10 mM) and unlabeled peptides (2.5 mM) were prepared. For a typical ESR measurement, the total lipid concentration was fixed at 10 mM and the peptide concentration was varied to obtain various ratios of peptide/lipid in a total volume of 50 μl. The membrane phase transition of liposomes of different composition was investigated by using a differential scanning colorimeter. The results show that the phase transition was not observed in the temperature region used for the current experiment (25°C) (data not shown).

Preparation of peptides

Custom peptides, C8-CB1, C32-CB1, C5-CB3, and C30-CB3, were synthesized by a 431 peptide synthesizer (Applied Biosystems, Foster City, CA) as described previously (Chen et al., 1997). The sequences of C8-CB1 and C32-CB1 were derived from CB1, except that the Ile at position 8 or 32 was replaced by Cys. The circular dichroism spectra of CB1, C8-CB1, and C32-CB1 show that all peptides form secondary structures in the helix-promoting solvent. More wild-type helical content as compared with its analogs was obtained (data not shown). Similarly, C5-CB3 and C30-CB3 were derived from CB3, with the Leu at position 5 or 30 replaced by Cys (see Fig. 1 for details). The molecular weight (MW) and purity of the various peptides were determined by mass spectrometry and HPLC. The results showed that MW/purity are 4107.61/99.0% for C8-CB1, 4106.97/96.7% for C32-CB1, 3548.79/95.6% for C5-CB3, and 3548.49/95.7% for C30-CB3. These data agree well with the sequences. The concentration of the peptide in PBS was determined by the bicinchoninic acid assay (Pierce Chemical Co., Rockford, IL).

Preparation of spin-labeled peptides

Each of the synthetic peptides, C8-CB1, C32-CB1, C5-CB3, or C30-CB3, in a degassed, 0.05 M acetate buffer at pH 4.5, was mixed with 5% (v/v) MTSSL in acetone. The molar ratio of MTSSL/peptide was 5 to 1. The mixtures were incubated at 25°C for 4 h. The labeled peptides (C8SL-CB1, C32SL-CB1, C5SL-CB3, or C30SL-CB3) were then separated from the free spin-label MTSSL by eluting them through Sephadex G-25 using PBS buffer at pH 7.4. Concentrations of the labeled peptides were determined by a micro BCA protein assay (Pierce Chemical Co.).

ESR spectroscopy

ESR spectra were recorded with a Varian E-109 X-band spectrometer (Palo Alto, CA) equipped with an E-231 TE-102 rectangular cavity. Experiments were done at 25°C maintained to $\pm$0.2°C using a nitrogen gas flow temperature regulation system. The exact temperature was measured with a thermocouple located at the bottom of the microwave cavity. Samples were prepared in 1-mm-ID sealed quartz capillaries accommodated within a standard 4-mm quartz ESR tube. ESR spectra were recorded at the frequency of 9.518 GHz using a microwave power of 10 mW. The magnetic field was centered at 3400 G and a field sweep of 100 G was used. A 100-kHz field modulation was applied with an amplitude of 0.8–1.25 G, depending on the spectral line width.

The ESR spectra of the DOXYL lipid spin label in PA/PC-CB1 and PA/PC-CB3 mixtures or in PA/PC lipids alone were recorded at constant temperature and pH. Spectral hyperfine splittings were determined by fitting the maximum and minimum in the outer wings of the spectrum to a Gaussian curve. The field difference between the two extremes was then calculated (see Fig. 2 *a*). The effective order parameter, S^{eff}, was determined by

$$S^{\mathrm{eff}} = \left(\frac{2A_{\mathrm{max}} - 2A_{\perp}}{2A_{\mathrm{zz}} - A_{\mathrm{xx}} - A_{\mathrm{yy}}}\right)(a_{\mathrm{o}}'/a_{\mathrm{o}}), \qquad (1)$$

where $2A_{\mathrm{max}}$ denotes the maximum outer ^{14}N-hyperfine splitting (see Fig. 2 *a*); and a_{o} and a_{o}' are given by $\frac{1}{3}(A_{\mathrm{max}} - 2A_{\perp})$ and $\frac{1}{3}(A_{\mathrm{xx}} + A_{\mathrm{yy}} + A_{\mathrm{zz}})$, respectively. $A_{\mathrm{xx}} = 5.9$ G, $A_{\mathrm{yy}} = 5.4$ G, and $A_{\mathrm{zz}} = 32.9$ G, are the principal values of the ^{14}N-hyperfine coupling tensor of doxylpropane (Jost et al., 1971). $A_{\perp}$ was obtained by (Gaffney, 1976)

$$A_{\perp} = 1.4\left(1 - \frac{2A_{\mathrm{max}} - 2A_{\mathrm{min}}}{2A_{\mathrm{zz}} - A_{\mathrm{xx}} - A_{\mathrm{yy}}}\right) + A_{\mathrm{min}}, \qquad (2)$$

where $2A_{\mathrm{min}}$ is the inner ^{14}N-hyperfine splitting (see Fig. 2 *a*).

In the gel phase of phospholipid bilayer membranes, $2A_{\mathrm{max}}$ is an essential parameter to characterize the chain dynamics. In the fluid phase,

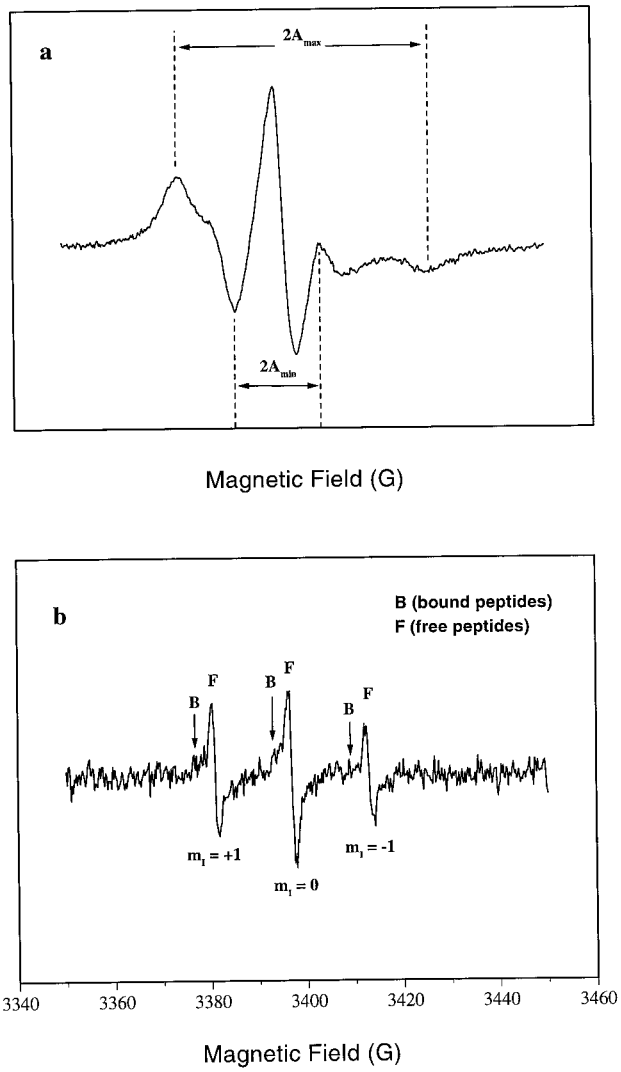

FIGURE 2 Spin-labeled ESR spectra. (*a*) Typical ESR spectrum of spin-labeled PC lipid. $2A_{max}$ and $2A_{min}$, indicating the maximum (outer) and the minimum (inner) hyperfine splittings, respectively, are defined. (*b*) Typical ESR spectrum of spin-labeled CB1 or CB3 peptide. $m_I = +1$, $m_I = 0$, and $m_I = -1$ denote the assignment of the three resonance lines to ^{14}N nuclear spin quantum number. F and B originate from free peptide (sharp) and peptides bound to lipid bilayer (broad), respectively.

both $2A_{max}$ and S^{eff} can be used as parameters to characterize the chain mobility at different positions of the probe. We have used these spectral parameters to compare the bilayer systems with or without CB1 and CB3.

Similar experimental conditions to those used for the spin-labeled lipids were applied to the study of the spin-labeled peptides. The rotational correlation time, τ_c, was expressed in terms of the relationship (Keith et al., 1970),

$$\tau_c = \left(\frac{120}{b}\right)(15b - 32\Delta\gamma H_o)^{-1}\left[\frac{T_2(0)}{T_2(-1)} - 1\right]T_2(0)^{-1}, \qquad (3)$$

where H_0 is the strength of the magnetic field; $T_2(0)$ and $T_2(-1)$ are the transverse relaxation times of $m_I = 0$ and $m_I = -1$ hyperfine components (for reference, see Fig. 2 *b*); $b = 4\pi/3\ [A_{zz} - \frac{1}{2}(A_{xx} + A_{yy})]$; and $\Delta\gamma = (\beta_e/\eta)\ [g_z - \frac{1}{2}(g_x + g_y]$. The transverse relaxation time $T_2(0)$ was taken from the linewidth of the ESR spectrum, and the ratio of T_2 values was taken from the relative peak height intensities.

For a spin-labeled peptide in the presence of lipid bilayers, the observed ESR spectrum often consists of a very sharp component (indicating high mobility; see F in Fig. 2 *b*) superimposed on a broader component (indicating lack of mobility; see B in Fig. 2 *b*). The sharp component corresponds to the free peptides in solution, whereas the broad component originates from membrane-bound peptides. The height of F at $m_I = -1$ could be quantitatively used to determine the fraction of the free-to-bound peptides in the liposomal solution. The amount of bound peptides was then calculated by the fraction of the free peptides multiplied by the known concentration of peptides in the sample (Castle and Hubbell, 1976). Specifically, the MTSSL spin-labeled peptides at a concentration of 20 μM were titrated with unlabeled liposomes of different compositions. An ESR spectrum for a known concentration of spin-labeled peptides (C_p) without lipids was taken and the peak height of the high-field line (h) was recorded. It is reasonable to assume that the amplitude of the peak height is proportional to the concentration of the free peptides (Keith et al., 1970). Under the same concentration of spin-labeled peptides with lipids, the peak height of the high-field line (h') in the ESR spectrum was again measured. The free peptide concentration, C_f, was determined by $C_f = C_p(h'/h)$. The molar ratio of the associated peptides (χ_b) was then obtained: $\chi_b = (C_p - C_f)/C_l$, where C_l is the stoichiometric lipid concentration. Plots of χ_b versus C_f can be used to investigate the binding cooperativity of the peptides to the lipid bilayers (Schwarz et al., 1986). If this binding isotherm exhibits a sigmoidal shape, one could obtain a critical peptide concentration, C_f^*, from the sharp increase in the slope of the curve.

Power saturation of ESR

For the power saturation experiments, samples were loaded into a capillary fabricated from gas-permeable plastic (Wilmad Glass Co., Inc., Buena, NJ). Before measurements, oxygen in the sample's tube was removed by passing nitrogen around the capillary for at least 20 min. Various concentrations of Crox, a relaxing agent (Berg and Nesbitt, 1979; Yager et al., 1979), were included in the peptide samples. The collisions of Crox with the spin-labeling probe, namely the nitroxide, result in a Heisenberg exchange (Molin et al., 1980) and thus broaden its ESR spectrum. The spin-lattice relaxation rate, $1/T_1$, for Crox is much faster than that for the nitroxide. The advantage of using Crox as a relaxer arises from its high insolubility in the membrane interior, and hence its ability to relax only nitroxides exposed to the aqueous phase.

Crox was used for two different kinds of measurements. 1) A high concentration of Crox (50 mM) in peptide solution was used to broaden the ESR spectrum of nitroxide exposed to the aqueous phase. The change of signal amplitude at $m_I = -1$ with and without Crox should reflect the extent to which the peptide is free in solution (i.e., unbound) or bound to the bilayer–aqueous interface but still exposed (see the Results section). Accordingly, binding and nonbinding peptides to the lipid membrane can be classified. 2) Different contents of Crox (5, 10, and 25 mM) in peptide solutions were used to determine the collision rate of the nitroxide with Crox. The collision rates can be measured by investigating the Heisenberg exchange rate and the effect on the spectral line shape (Molin et al., 1980). The observed transverse spin relaxation time is related to the concentration of Crox as follows (Subczynski and Hyde, 1981):

$$(T_2)_{obs}^{-1} = (T_2^0)^{-1} + C[\text{Crox}], \qquad (4)$$

where T_2 and T_2^0 are the nitroxide transverse spin relaxation times in the presence and absence of Crox, respectively. The constant of proportionality, C, provides a measure of nitroxide accessibility as well as the collision rates.

Continuous wave (CW) ESR power saturation can be used to obtain the half saturation parameter, $P_{1/2}$, the microwave power required to saturate the signal to one-half of the amplitude when the spectral line is nonsaturated. For a single homogeneous Lorentzian line, the peak-to-peak amplitude of the first derivative absorption spectrum, Y', has been derived by Poole (1983) as follows.

$$Y' = KP^{1/2}(1 + P/P_{1/2})^{-1.5}, \qquad (5)$$

where K is a proportionality constant and P is the microwave power. The half saturation parameter in the absence ($P^0_{1/2}$) and presence ($P_{1/2}$) of Crox can be expressed as

$$P_{1/2} = P^0_{1/2} + C'[\text{Crox}]. \quad (6)$$

Again, C' is a parameter that reflects the accessibility of the spin label to the relaxer, Crox; specifically, C' is related to C/T^0_2 (see Eq. 4). A plot of $P_{1/2}$ versus [Crox] gives the slope, C' and the intercept, $P^0_{1/2}$. For each concentration of Crox, the peak height of the $m_I = 0$ line was measured by gradually increasing the power. $P_{1/2}$ was obtained by fitting the curve of the first derivative of the signal amplitude versus the square root of power (for example, see Fig. 10 *a*) using Eq. 5. The fitting process was performed using nonlinear least-square regression.

RESULTS

ESR spectra of spin-labeled lipid chains in the presence of CB1 and CB3

Lipid chain mobility

The effects of CB1 and CB3 on the lipid chain mobility of liposomes at the lipid/peptide molar ratio of 500/1 are shown for various DOXYL spin-labeled lipids, 5′SL-PC, 7′SL-PC, 10′SL-PC, 12′SL-PC, and 16′SL-PC in Fig. 3. Liposomes of two different lipid compositions were studied: $\beta = 0.25$ and $\beta = 0.75$. Panels a and b compare the ESR spectra of the spin-labeled probes at 25°C in the presence (*solid lines*) and absence (*dotted lines*) of CB1 and CB3 peptides, respectively.

Broader resonances and larger splittings of the spectra are observed for all spin-labeled liposomes in the presence of CB1 than those observed for CB3-liposome solutions and lipid alone, except in the case of 16′SL-PC, where all peptides exhibited similar spectra. Table 1 summarizes the measured values of $2A_{max}$ of different spin-labeled lipids in $\beta = 0.25$ and $\beta = 0.75$ liposomes in the presence of CB1 and CB3. The biggest perturbation of lipid mobility at $\beta = 0.25$, upon adding CB1 and CB3, is at the 10′ position of PC, with $\Delta 2A_{max}$ of 1.4 and 0.8 Gauss, respectively. For $\beta = 0.75$ liposomes, the largest perturbation by CB1 also occurs at the 10′ position of PC with $\Delta 2A_{max}$ of 4.1 Gauss. Thus, a large increase in the maximum outer hyperfine splittings, $2A_{max}$, of the DOXYL spin label in $\beta = 0.75$ liposomes relative to those in $\beta = 0.25$ liposomes was seen on CB1 binding. In the case of CB3, the 7′ and 12′ positions

TABLE 1 The maximum outer hyperfine splitting ($2A_{max}$, Gauss) observed for the various spin-labeled lipids at different positions along the acyl chain in the absence and presence of CB1 and CB3 peptides in PA/PC liposomes of composition $\beta = 0.25$ and 0.75*

	Lipid Alone	CB1	$\Delta 2A_{max}$	CB3	$\Delta 2A_{max}$
$\beta = 0.25$					
5′-PCSL	26.3	26.7	0.4	26.2	−0.1
7′-PCSL	25.0	25.8	0.8	24.9	−0.1
10′-PCSL	21.8	23.2	1.4	22.6	0.8
12′-PCSL	19.7	19.6	−0.1	19.2	−0.5
16′-PCSL	16.4	16.1	−0.3	16.3	−0.1
$\beta = 0.75$					
5′-PCSL	25.8	28.6	2.8	25.9	0.1
7′-PCSL	24.6	27.3	2.7	25.6	1.0
10′-PCSL	22.1	26.2	4.1	22.0	0.1
12′-PCSL	19.0	23.0	4.0	20.0	1.0
16′-PCSL	16.6	16.5	0.1	16.4	0.2

*β = (PA)/(PC + PA) molar fraction.
The value of $\Delta 2A_{max}$ in each entry corresponds to the difference of $2A_{max}$ between CB1 or CB3 and lipid alone. The peptide and lipid concentrations used in these experiments were 20 μM and 0.1 mM, respectively. All spectra were recorded at room temperature.

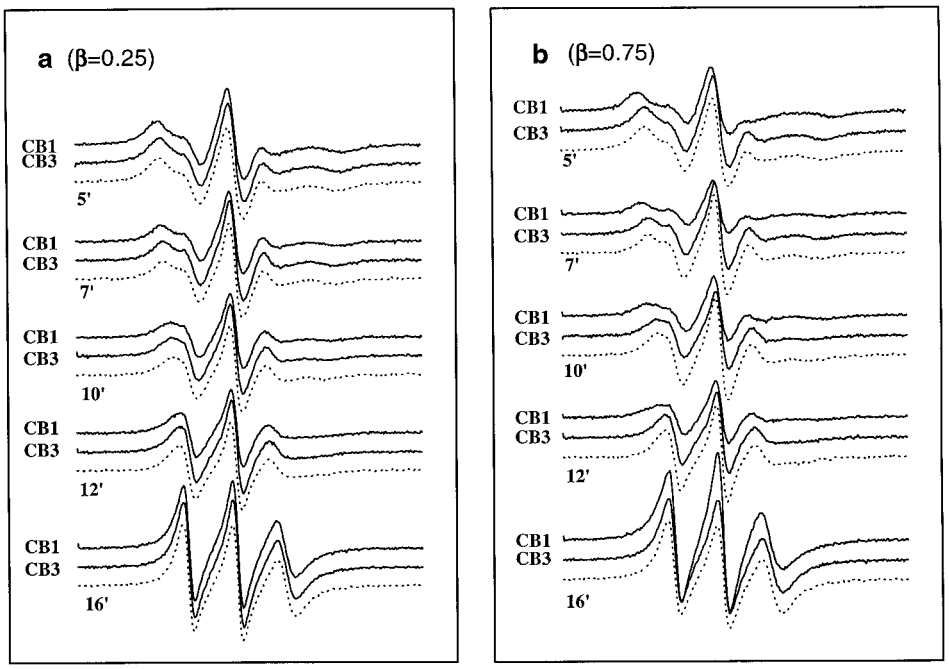

FIGURE 3 Effect of CB1 or CB3 peptides on the spectra of spin-labeled lipids. Spectra of the DOXYL lipid spin-label with the label at a various positions along the acyl chain of PC (5′, 7′, 10′, 12′, and 16′) in (*a*) $\beta = 0.25$ liposomes, and (*b*) $\beta = 0.75$ liposomes. *Solid line:* spectra obtained with the addition of peptides; *dashed line:* control without peptides. The field scan width is 100 Gauss. The temperature of the samples was maintained at 25°C.

of PC showed the largest changes ($\Delta 2A_{max}$ = 1.0 Gauss) for β = 0.75. However, the extent of perturbation on lipid bilayers induced by CB1 is much higher than that by CB3 ($\Delta 2A_{max}$ = 0.60 Gauss, on average, for CB1, and 0.32 Gauss for CB3 at β = 0.25; and $\Delta 2A_{max}$ = 2.74 Gauss, on average, for CB1 and only 0.48 Gauss for CB3 at β = 0.75). Accordingly, we conclude that there is a restriction of the motion of the spin-labeled chains in the presence of CB1, whereas the effect of the binding CB3 on lipid chain mobility was not significant.

Figure 4, *a* and *b*, shows plots of S^{eff} versus n'SL-PC (n' = 2, 7, 10, 12, and 16) for liposomes at β = 0.25 and β = 0.75, respectively. As expected, the calculated S^{eff} decreases with the nitroxide position, n', as the position of the nitroxide probe in the lipid chain becomes further removed from the polar head. A similar dependence of $2A_{max}$ was also observed (see Table 1). These results are consistent with increased immobilization of hydrocarbon chains near the polar headgroups than toward the tail. In fact, the segmental flexibility at position 16′ is identical for all peptides. The S^{eff} of the spin probe in the presence of CB1 is otherwise larger than in the case of CB3 over the bulk of the acyl chain for both lipid compositions studied. It is interesting to note that the steepest change in the flexibility gradient is shifted toward the bilayer interior from positions 10′ to 12′ of the *sn*-2 acyl chain in β = 0.75 liposomes upon binding CB1 (see Fig. 4 *b*), suggesting an overall stiffening of the bilayer under these conditions.

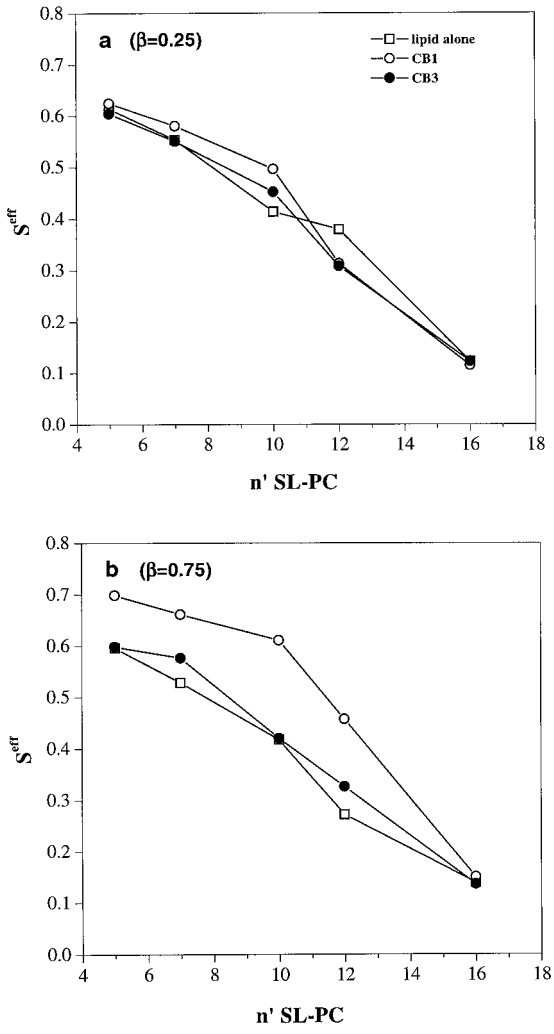

FIGURE 4 Effective order parameters as a function of the nitroxide position. The S^{eff} for the various n'SL-PC was calculated using Eq. 1 shown in the text. The dependence of S^{eff} on the positions of the DOXYL lipid spin-label along the chain of the n'SL-PC is shown in (*a*) for β = 0.25 liposomes and (*b*) for β = 0.75 liposomes for the various peptides: CB1 (*open circles*); CB3 (*filled circles*); and lipid control (*open squares*). All experiments were undertaken at 25°C.

Bilayer binding affinities of CB1 and CB3

The spin-labeled lipids exhibiting the largest $\Delta 2A_{max}$ (10′SL-PC for CB1/CB3 at β = 0.25 and CB1 at β = 0.75; 7′SL-PC for CB3 at β = 0.75; see Table 1) were selected for further study of the relationship between $2A_{max}$ and the molar ratio of peptide/lipid. Figure 5, *a* and *b*, shows the influence of CB1 and CB3, respectively, at different peptide/lipid ratios, on the spin-labeled liposomes for β = 0.25 and β = 0.75. These results showed that the degree of motional averaging decreases dramatically ($2A_{max}$ increases) when more CB1 is added into the bilayer membrane (see Fig. 5 *a*). The amount of CB1 needed to saturate the $2A_{max}$ response of DOXYL in the lipid bilayers (CB1/lipid; mol/mol) is lower at β = 0.25 (0.1 mol/mol) than at β = 0.75 (0.25 mol/mol). However, the perturbation amplitude ($\Delta 2A_{max}$) is smaller with CB1 at β = 0.25 (1.91 Guass from 0 to 0.1 mol/mol) than at β = 0.75 (5.5 Gauss from 0 to 0.25 mol/mol). As a measure of the binding stochiometry at saturation, we have taken the intercept of the initial slope in $2A_{max}$ with the plateau value shown in Fig. 5. The lipid/peptide molar ratios are approximately 17 and 7 lipids per CB1, respectively, for liposomes at β = 0.25 and β = 0.75. In contrast, the perturbation of lipid mobility of the bilayer membranes was not dramatically affected by the association of CB3 (see Fig. 5 *b*). The perturbation amplitudes ($\Delta 2A_{max}$) are significantly smaller, by a factor of 2 or 4, than in the case of CB1. Clearly, the association of CB3 with lipid bilayers, unlike CB1, is weak.

Interactions of MTSSL spin-labeled CB1 and CB3 with lipid bilayers

Binding of peptides to lipid bilayers

Typical ESR spectra of MTSSL spin-labeled peptides, C8SL-CB1, C32SL-CB1, C5SL-CB3, and C30SL-CB3 in PBS are shown in Fig. 6 *a*, *(1)-(4)*, respectively. Three sharp peaks were observed for all labeled peptides. This observation indicates that the peptides undergo very rapid and independent motions of their individual segments. Fig. 6 *b* shows the corresponding ESR spectra of the spin-labeled peptides upon the addition of β = 0.25 liposomes. The mobility of C8SL-CB1 and C32SL-CB1 either in aqueous

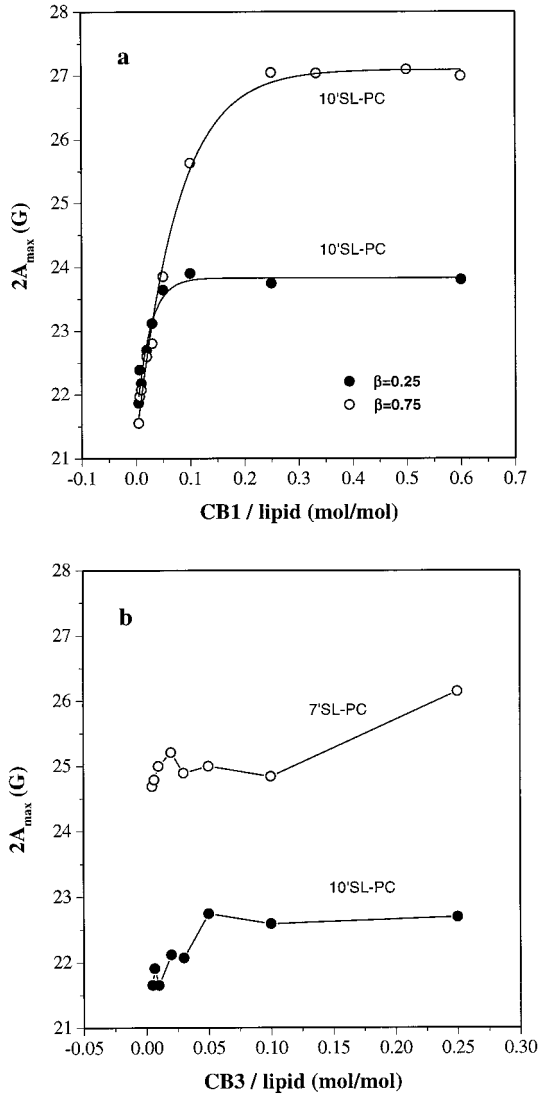

FIGURE 5 Dependence of the maximum outer hyperfine splittings on the molar ratio of peptides to lipid. (*a*) $2A_{max}$ of 10′SL-PC as a function of the molar ratio of CB1/lipids in $\beta = 0.25$ liposomes (*filled circles*); and in $\beta = 0.75$ liposomes (*open circles*). (*b*) $2A_{max}$ of 10′SL-PC as a function of the molar ratio of CB3/lipids in $\beta = 0.25$ liposome (*filled circles*); and $2A_{max}$ of 7′SL-PC as a function of the molar ratio of CB3/lipids in $\beta = 0.75$ liposome (*open circles*).

solution or in the solution with liposome could correlate to $1/\tau_c$ (Eq. 3). For free-bound peptides (bound state of Fig. 6, *a* or *b*), τ_c estimated from *F* component is similar (~0.5 ns) for both C8SL-CB1 and C32SL-CB1. However, τ_c for lipid-bound C8SL-CB1 and C32SL-CB1, shown in Fig. 6 *d* are different (~1.5 and 1.8 ns, respectively). The longer τ_c implies a lower mobility. The issue of forming a secondary structure of peptides on the change of ESR spectrum may not be significant in this experiment. It was observed that the ESR spectra of panels a (unfolded) and b (folded) for C30SL-CB3 are almost identical. Changes of ESR could therefore be due to other factors such as characteristics of the helix, bound state, etc. The residual spectrum shown in Fig. 6 *c(4)*, is not clear. It may be due to the complex aggregation between CB3 and lipids.

In this experiment, the ratio of lipid to peptide is 100 to 1, which is far greater than the lipid/peptide binding stoichiometry (17 to 1, see Fig. 5 *a*). For the MTSSL spin-labeled CB1 derivatives, C8SL-CB1 (Fig. 6 *b(1)* and C32SL-CB1 (Fig. 6 *b(2)*), each spectrum is a composite of different subspectra arising from a population of peptides with different rotational mobility. The sharp component, *F*, shown in Fig. 6 *b, (1)* and *(2)* is smaller compared with that shown in Fig. 6 *a, (1)* and *(2)*. This indicates that the amount of free peptides in solution has been reduced significantly in the presence of the liposomes. Clearly, the remaining broadened peaks arise from the peptides bound to the lipid membrane. Finally, the lower amplitudes of the high-field lines of C32SL-CB1 (Fig. 6 *b(2)*) when compared with those of C8SL-CB1 (Fig. 6 *b(1)* suggest that the COOH-terminal helix is more immobilized, or binds more tightly to the lipids than does the NH_2-terminal helix. This result indicates that the COOH-terminal helix may be buried within the inside of the lipid bilayers. In contrast, the spectra of MTSSL spin-labeled CB3 derivatives, C5SL-CB3 (Fig. 6 *b(3)* and C30SL-CB3 (Fig. 6 *b(4)*, are similar to that of the free peptides (see Fig. 6 *a, (3)* and *(4)*). Again, these results may be taken as evidence that CB3 binds only marginally to the lipid bilayer.

To determine whether the individual labeled peptides are buried within the membrane or are physically adsorbed at the aqueous–membrane interface, 50 mM Crox was added to the peptide–liposome solutions. Crox is a hydrophilic paramagnetic compound that collides effectively with the nitroxide and causes relaxation of the nitroxide electron spin. A mixture of Crox with MTSSL has been demonstrated to accelerate electron relaxation and broaden the ESR spectrum of the nitroxide. The charged Crox cannot diffuse into the hydrophobic region of the bilayer, and, therefore, this relaxation broadening could be used to probe the details of the mode of binding of the various peptides to the membrane. Fig. 6 *d, (1)* to *(4)*, show the ESR spectra of Crox with the spin-labeled peptides, C8SL-CB1, C32SL-CB1, C5SL-CB3, and C30SL-CB3, respectively, in the presence of liposomes. As control, the ESR spectra of the corresponding spin-labeled peptides in the presence of Crox alone are shown in Fig. 6 *c*. A comparison between the data summarized in Fig. 6 *c, (1)* and *(2)* and 6 *d, (1)* and *(2)*, clearly indicates that some CB1 is buried into the hydrophobic region of the membrane, because relatively broad resonances are observed for the spin-labeled peptide in the presence of liposome (see Fig. 6 *d, (1)* and *(2)*. In contrast, for the MTSSL spin-labeled CB3 derivatives, the ESR signals of the corresponding nitroxides are essentially identical in the absence (see Fig. 6 *c, (3)* and *(4)* and presence (see Fig. 6 *d, (3)* and *(4)* of liposomes, both in terms of signal intensity and spectral widths. These observations indicate that both C5SL-CB3 and C30SL-CB3 were preferentially partitioned in the aqueous solution ($\beta = 0.25$). However, the partitioning of CB3 peptides is membrane-composition dependent. For $\beta = 0.75$ and $\beta = 1.0$ liposomes, we have obtained ESR spectra that

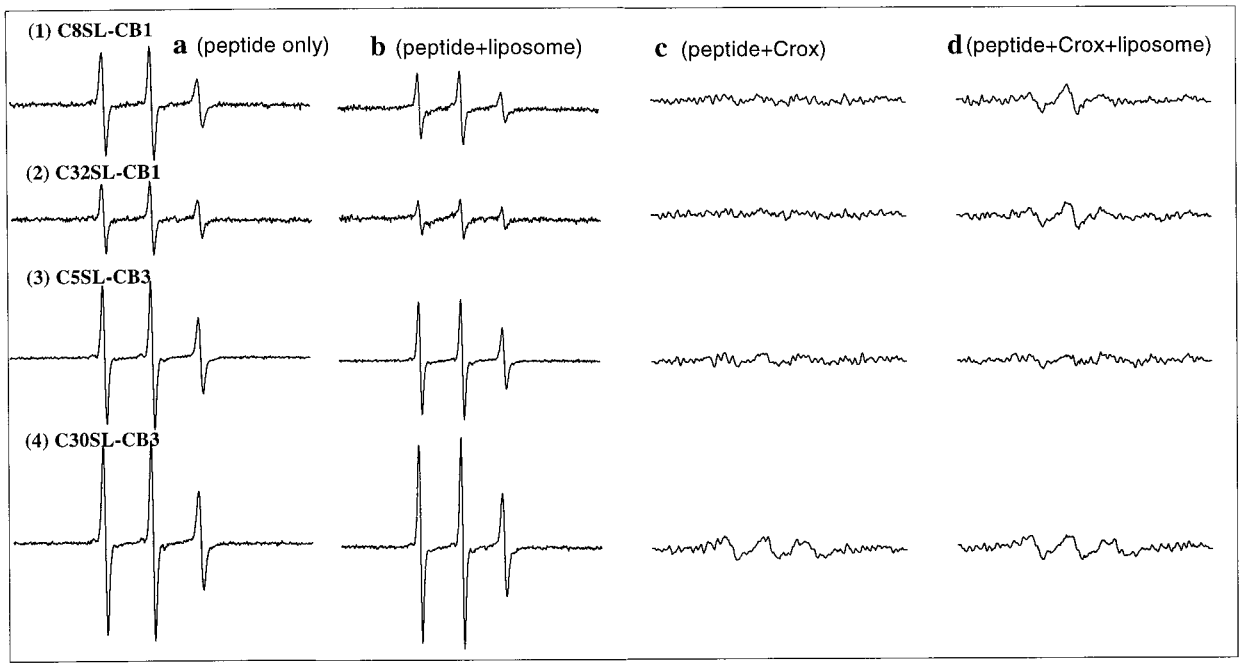

FIGURE 6 ESR spectra of spin-labeled peptides. *(1)*, C8SL-CB1; *(2)*, C32SL-CB1; *(3)*, C5SL-CB3; and *(4)*, C30SL-CB3 in (*a*) aqueous solution; (*b*) $\beta = 0.25$ liposomes; (*c*) 50 mM Crox; and (*d*) $\beta = 0.25$ liposomes and 50 mM Crox.

suggest that C5SL-CB3 may also insert into the hydrophobic core of the lipid bilayers (data not shown).

Binding affinity of peptides to lipid bilayers

Figure 7, *a* and *b*, depicts the amount of spin-labeled CB1 and CB3 (χ_b) bound to liposomes of varying βs. C8SL-CB1 and C32SL-CB1 peptides display exponential increases in the amount of bound peptides when the PA content in the liposomes is increased (Fig. 7 *a*). For the MTSSL-labeled CB3 derivatives, C5SL-CB3 and C30SL-CB3, the results are significantly different (Fig. 7 *b*). The data suggest that the COOH-terminal helix of C30SL-CB3, where the spin label is located, does not seem to bind at all to the lipid bilayer, even when the liposomes contain an unusually high content of PA. In contrast, the NH_2-terminal helix in C5SL-CB3, where the spin label is located in this derivative, exhibits two stages of binding to the lipid bilayer: below $\beta = 0.2$, the number of bound peptides reduces as the content of PA in liposomes increases; above $\beta = 0.2$, the amount of CB3 bound to the lipids increases linearly as more PA is incorporated into the liposomes. For the view of the overall peptide, a slower tumbling upon the binding of peptides with lipid bilayers may be foreseen.

Binding isotherms of peptides to lipid bilayers

To characterize the binding affinity of the peptides to lipid membranes, the MTSSL-labeled CB1 and CB3 derivatives (at a concentration of 20 μM) were titrated with varying concentrations of $\beta = 0.25$ and $\beta = 0.75$ liposomes (the initial concentration was 10 mM). The molar ratio of the bound peptides to the lipid bilayers (χ_b) was determined based on the amplitude of the high-field resonance of the spectra of the spin-labeled peptides at each concentration of the lipids. The binding isotherms were analyzed in terms of a partition equilibrium. Schwarz et al. (1986) reported that the shape of a binding isotherm of a peptide can provide information on the cooperativity of binding to the lipid bilayer.

Plots of the molar ratio, χ_b, of the bound peptides versus the free peptide concentration (C_f) for C8SL-CB1, C32SL-CB1, C5SL-CB3, and C30SL-CB3, at $\beta = 0.25$ and $\beta = 0.75$ liposomes are shown in Fig. 8, *a–d*, respectively. For spin-labeled CB1 derivatives, C8SL-CB1 (Fig. 8 *a*) and C32SL-CB1 (Fig. 8 *b*), the binding isotherms reveal sigmoidal shapes, implying positive cooperativity. The effect is more significant in $\beta = 0.75$ liposomes than in $\beta = 0.25$ liposomes for both C8SL-CB1 and C32SL-CB1. A higher plateau of χ_b in $\beta = 0.75$ liposomes was also obtained for both spin-labeled CB1 peptides. This indicates a stronger affinity of CB1 to the lipids as the amount of the negatively charged lipids is increased. Also, the χ_b of C8SL-CB1 for either $\beta = 0.75$ or $\beta = 0.25$ liposomes (Fig. 8 *a*) is higher than that of C32SL-CB1 (Fig. 8 *b*). This observation would seem to suggest that the COOH-terminal helix penetrates into the hydrophobic core of the membrane and MTSSL-labeling at Cys^{32} interferes somewhat with this binding. Presumably, the NH_2-terminal helix of the CB1 rests on the membrane–aqueous interface.

For the binding of CB3 to lipids, the results are different. Only one sigmoidal binding isotherm was observed for C5SL-CB3 in $\beta = 0.75$ liposomes (Fig. 8 *c*). The remaining

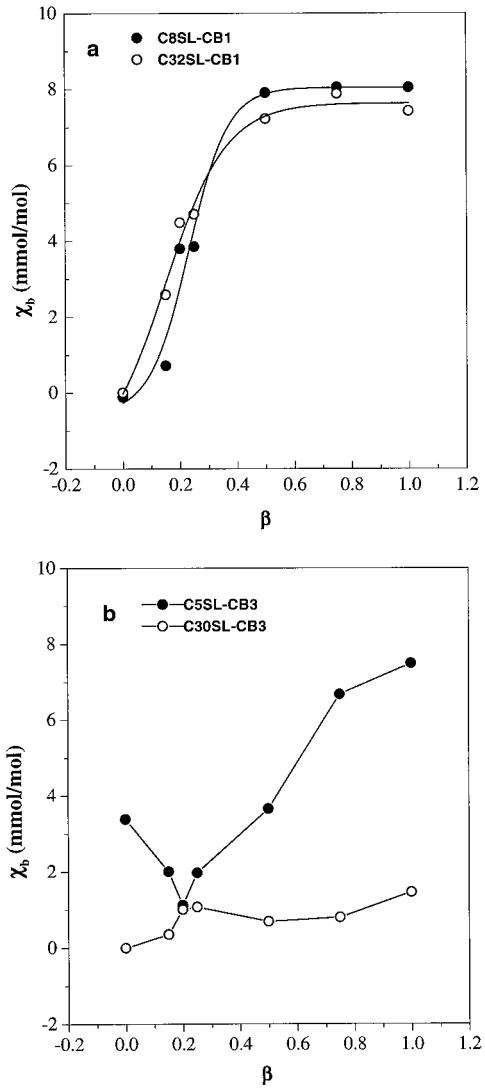

FIGURE 7 Binding affinity of the associated peptides with the PA content in the liposome. The molar ratio (χ_b) of the associated peptides to the lipid was measured as a function of β. (*a*) C8SL-CB1 (*filled circles*) and C32SL-CB1 (*open circles*); (*b*) C5SL-CB3 (*filled circles*) and C30SL-CB3 (*open circles*). The experiments were conducted on samples containing 20 μM spin-labeled peptides and 2 mM nonspin-labeled lipids.

binding isotherms, including those for C5SL-CB3 in β = 0.25 liposomes (Fig. 8 *c*) and C30SL-CB3 in both β = 0.25 and β = 0.75 liposomes (Fig. 8 *d*), indicate negligible binding of the peptides-to-lipid bilayers.

The apparent critical aqueous concentration, C_f^*, offers a measure of the amount of free peptide in equilibrium with a saturated monolayer of membrane-bound peptide. This quantity can be inferred from the sigmoidal curves depicted in Fig. 8, *a–c*: 15 μM and 8 μM for C8SL-CB1 in β = 0.25 and β = 0.75 liposomes, respectively; and 11 μM and 12 μM for C32SL-CB1 in β = 0.25 and β = 0.75 liposomes, respectively. Thus, for C8SL-CB1, C_f^* is reduced from 15 μM to 8 μM as the PA content is increased from (β = 0.25 to β = 0.75). In other words, C8SL-CB1 shows a stronger affinity for PA compared to PC. In contrast, the C_f^* of C32SL-CB1 remains almost unchanged for both β = 0.25 and β = 0.75 liposomes. However, because C_f^* for a given membrane composition must be the same for a given unlabeled peptide, the apparent disparity must reflect subtle effects arising from the perturbation of physical chemistry of the interaction between the COOH-terminal helix and the membrane introduced by the bulky nitroxide probe.

Aggregation state of bound peptides

To ascertain whether the observed cooperativity in the binding is due to aggregation of the peptides within the membrane, ESR experiments were performed on the peptides bound to acidic liposomes (β = 1.0) at two peptide/lipid ratios, 1/50 and 1/10. The peptide solution at the higher concentration (peptide/lipid ratio of 1/10) was prepared by adding appropriate amounts of unlabeled CB1 or CB3 derivatives to the 1/50 spin-labeled peptide/lipid solution. The use of unlabeled peptides to enhance the peptide concentration obviates any effects on the broadening of the ESR line widths from spin–spin interactions, which might otherwise occur when labeled peptide is used. If the peptides are aggregated in the membrane, the line widths of the ESR spectra may become broader because of a reduction in the rotational correlation time of the aggregated peptides (Archer et al., 1991). Figure 9, *a–c*, compares the results of MTSSL-labeled peptides, C8SL-CB1, C32SL-CB1, and C5SL-CB3, respectively, at peptide/lipid ratios of 1/50 (*curves i*) and 1/10 (*curves ii*) in 1 mM liposomes of β = 1.0 and 50 mM Crox (to eliminate the ESR signals arising from free and unbound peptide). Despite the difference in signal intensity of the spectrum of C8SL-CB1 between *(i)* and *(ii)* in Fig. 9 *a*, the spectral line shapes are virtually identical, i.e., the line width does not depend on the amount of peptides in the bilayer. Although this result might imply that CB1 does not aggregate in the membrane, we prefer to interpret these data to mean that the local motions of the nitroxide spin label are relatively insensitive to the state or details of aggregation of the peptides within the membrane. Similar results have been obtained for C32SL-CB1 and C5SL-CB3 peptides: here, the intensity and line widths of the spectra shown for both peptide/lipid ratios are almost identical (compare Fig. 9, *b* and *c*, respectively).

Accessibility of the bound peptides to aqueous solution

The interaction of Crox with nitroxide was investigated using the method of CW ESR power saturation. Peptide–liposome (β = 0.25) complexes were titrated with Crox at different concentrations.

To ensure that Crox relaxes only the membrane-bound spin label, two approaches were conducted: 1) High concentration of lipid (4 mM) was used to increase the amount of membrane-bound peptides, i.e., to decrease the amount of peptides free in solution, and 2) High concentration of Crox (5–15 mM) were used to remove any interference due to the peptides free in the aqueous phase. A relatively broad spec-

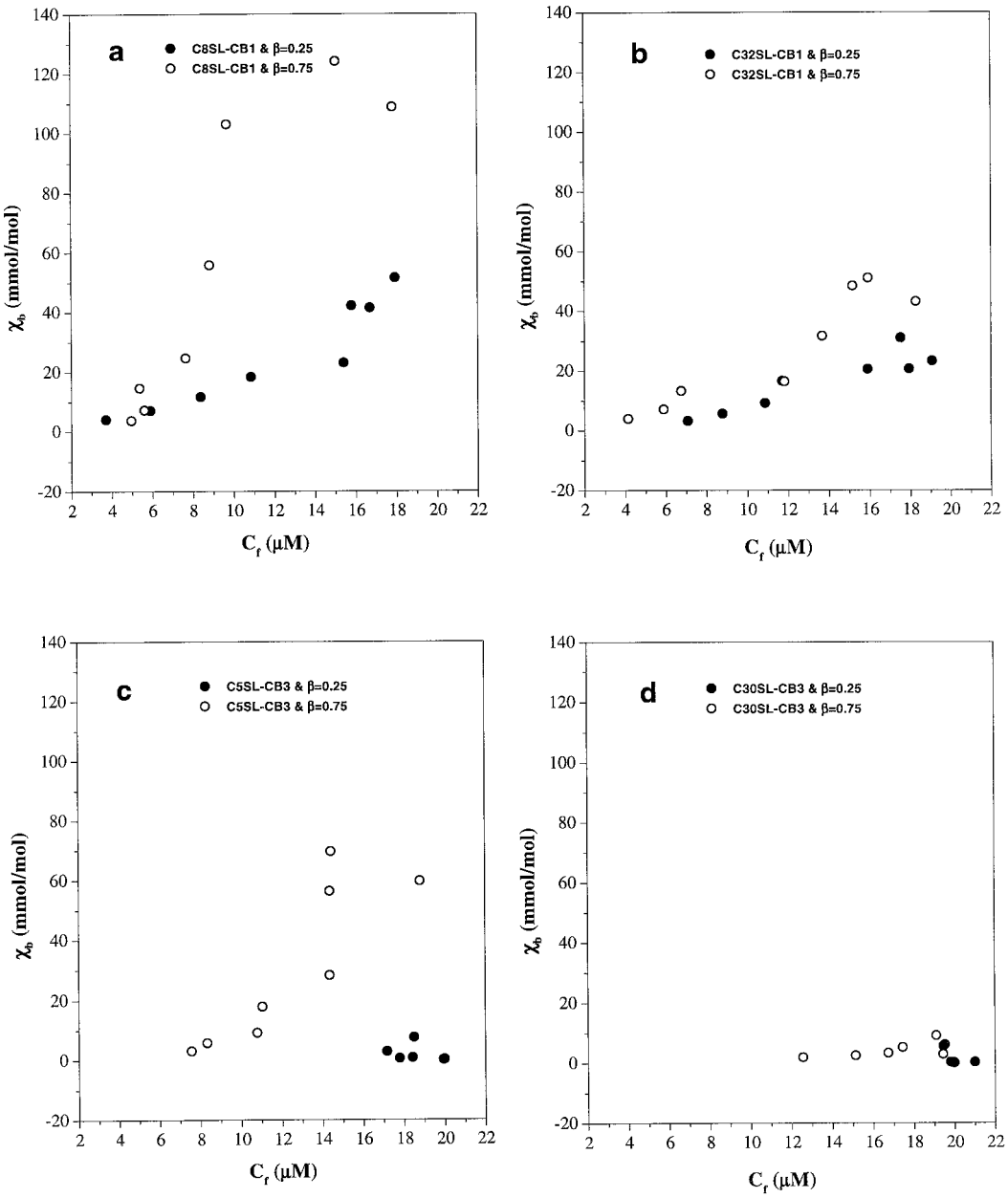

FIGURE 8 Equilibrium concentration of the associated peptides with the free peptide concentration. The molar ratio (χ_b) of the associated peptides to lipids (mmol to mol) is plotted as a function of the free peptide concentration (C_f) at equilibrium. (*a*) C8SL-CB1 at $\beta = 0.25$ (*filled circles*) and $\beta = 0.75$ liposomes (*open circles*); (*b*) C32SL-CB1 with $\beta = 0.25$ (*filled circles*) and $\beta = 0.75$ liposomes (*open circles*); (*c*) C5SL-CB3 with $\beta = 0.25$ (*filled circles*) and $\beta = 0.75$ liposomes (*open circles*), and (*d*) C30SL-CB3 with $\beta = 0.25$ (*filled circles*) and $\beta = 0.75$ liposomes (*open circles*). The total concentration of spin-labeled peptides was 20 μM in each of these experiments.

trum originated from membrane-bound peptides was shown (see inset of Fig. 10 *a*). A typical plot of the first derivative of the signal amplitude versus the square root of power for C32SL-CB1 is shown in Fig. 10 *a*. Based on the best fit (*solid lines* in Fig. 10 *a*), $P_{1/2}$ at different conditions were obtained. Plots of $P_{1/2}$ as a function of [Crox] for both C8SL-CB1 and C32SL-CB1 are shown in Fig. 10 *b*. The slopes, C', 24.9 mW/mM for C8SL-CB1 and 6.43 mW/mM for C32SL-CB1, reflect the relative measure of nitroxide accessibility to the aqueous phase (Eq. 6). It is evident that the effect of Crox on $P_{1/2}$ is larger for a nitroxide at the C8 residue of CB1 than for that at the C32 residue.

DISCUSSION

Perturbations of the lipid bilayer by peptides

The binding of CB1 to lipid bilayers causes a restriction of the lipid acyl chain motion as revealed by spectral broadening and increases in $2A_{max}$. The $2A_{max}$ reaches a plateau

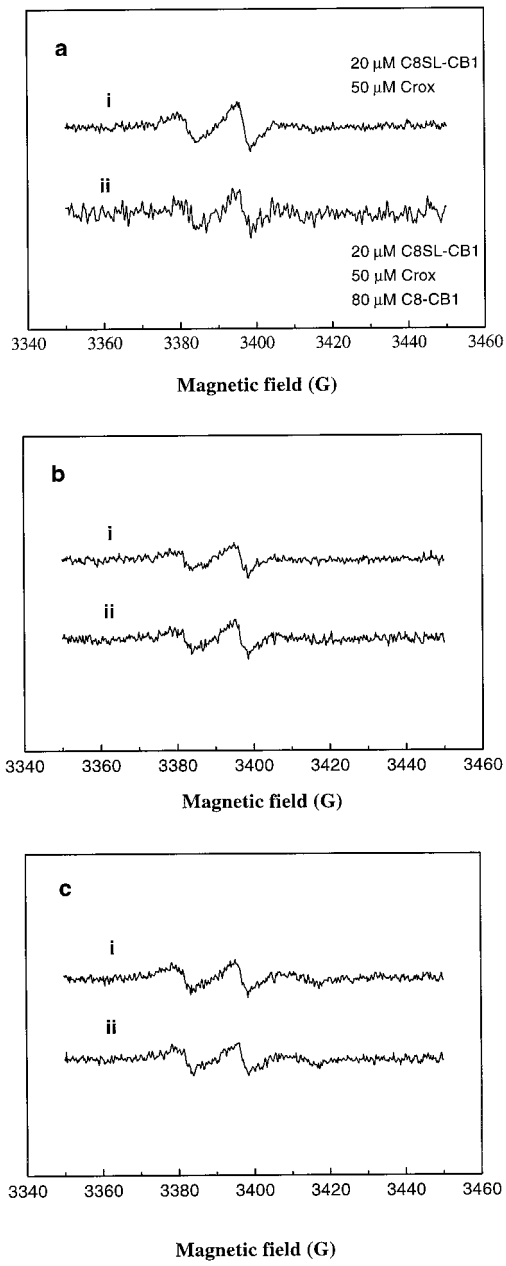

FIGURE 9 ESR spectra of spin-labeled peptides at different peptide/lipid ratios. The ESR spectra of the peptide-liposome dispersions at different peptide/lipid ratios of 1/50 and 1/10. The liposomes used in this experiment consist of 100% PA and the concentration of lipid is 1 mM. (*a*) 20 μM C8SL-CB1 and 50 mM Crox (*curve i*), and 20 μM C8SL-CB1 plus 80 μM C8-CB1 and 50 mM Crox (*curve ii*). (*b*) 20 μM C32SL-CB1 and 50 mM Crox (*curve i*), and 20 μM C32SL-CB1 plus 80 μM C32-CB1 and 50 mM Crox (*curve ii*). (*c*) 20 μM C5SL-CB3 and 50 mM Crox (*curve i*), and 20 μM C5SL-CB3 plus 80 μM C5-CB3 and 50 mM Crox (*curve ii*).

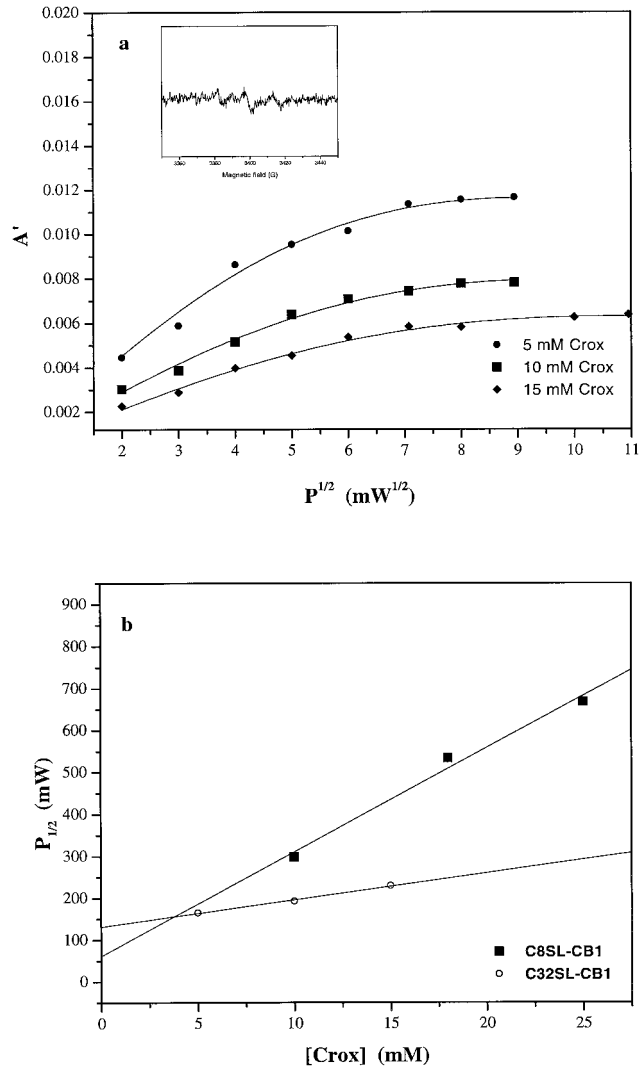

FIGURE 10 ESR power saturation of spin-labeled peptides as a function of Crox. (*a*) A typical example of the first derivative of the ESR signal amplitude (**A′**) versus the square root of microwave power ($P^{1/2}$) for C32SL-CB1 at $\beta = 0.25$. (*b*) Plots of $P_{1/2}$ versus the [Crox] for C8SL-CB1 and C32SL-CB1. The concentrations of spin-labeled peptides and non-spin-labeled lipids used for this experiment were 20 μM and 4 mM, respectively.

maximum at a peptide concentration that reflects the binding stoichiometry of the particular lipid-type for CB1 (Fig. 5 *a*). The plateau is reached at a lower bound peptide concentration for $\beta = 0.25$ liposomes than for $\beta = 0.75$ liposomes. In terms of binding stoichiometry, the plateau level corresponds to a molar lipid/peptide of 17 lipids per CB1 for $\beta = 0.25$ liposomes and 7 lipids per CB1 for $\beta = 0.75$ liposomes. These results most likely reflect the different capacity for binding CB1 for the two types of liposomes (different level of negative charge). However, differences arising from the membrane fluidity between the two liposomes cannot be ruled out.

For comparison, Kleinschmidt et al. (1997) reported lipid/peptide molar ratio of approximately 60 and 10 for the DMPC/melittin and DTPG/melittin complexes, respectively. Our earlier biosensor results (Wang et al., 1998) also indicated a stronger binding of CB1 to more acidic lipids ($K_a = 3.04 \times 10^{-4}\ M^{-1}s^{-1}$ for $\beta = 0.75$ liposomes and $K_a = 1.52 \times 10^{-4}\ M^{-1}s^{-1}$ for $\beta = 0.25$ liposomes). These results would seem to suggest that there is an electrostatic enhancement of peptide binding to lipid bilayers with a

higher anionic content for both CB1 and melittin (Terwilliger and Eisenberg, 1982), which have amphipathic α-helices. The stronger binding of peptides to the lipid headgroups may translate into greater motional restriction when the peptides bind to the lipid membranes (Wang et al., 1998).

In the case of CB3, with two hydrophobic α-helices and a net positive charge of 3, the binding interactions with the lipid bilayers are clearly different. Unlike CB1, which shows a clear trend in its interaction with lipids, CB3 shows only a weaker interaction with both $\beta = 0.25$ and $\beta = 0.75$ lipid bilayers (Fig. 5). Moreover, the data obtained for CB3 showed an irregular pattern. These observations support the suggestion that CB3 peptides cluster in the domains of the membrane enriched in lipid with neutral headgroups, namely, PC (Wang et al., 1998). The amplitude of the perturbation of lipid chain mobility ($\Delta 2A_{max}$) caused by CB3 is much smaller than that of CB1 (Table 1). We surmise that the lysis action induced by CB3 is different from that of CB1 and may not involve electrostatic binding with the anionic lipid in the bilayer.

Binding of CB1 and CB3 to lipid bilayers

To further understand the membrane binding of the peptides and their distributions in phospholipid bilayers, both CB1 and CB3 were spin-labeled at different positions, and their binding were examined. The results obtained suggest that the binding of spin-labeled CB1 to phospholipid bilayers is mediated to a large extent by electrostatic interactions. In $\beta = 0.25$ liposomes, the NH_2-terminal α-helix of CB1 may be parallel to the lipid bilayers (Fig. 6, *(1)a–(1)d*). From the power saturation study of spin-labeled CB1, we found that C8SL-CB1 is relaxed more easily by Crox than is C32SL-CB1 (Fig. 10 *b*). This latter observation suggests that the C8 residue resides near the membrane–aqueous interface, while C32 is embedded in the membrane. Altenbach et al. (1989) have applied this method to define the details of insertion spin-labeled bacteriorhodopsin into membrane. In the latter experiments, the spin label is attached to a transmembrane segment, so the accessibility to Crox should be limited and the change of $P_{1/2}$ in the presence of 50 mM Crox was not found to be significant. However, with our present system, significant changes in the $P_{1/2}$ were observed even though only 0.25 mM of Crox was used. Our results on CB1 provide clear evidence that the nitroxide on the two peptide derivatives studied here are at least partially accessible to water.

Mchaourab et al. (1994) have offered a schematic illustration of the cecropin AD-lipid bilayer (POPC and POPG) interaction in which the COOH-terminal α-helix is inserted into the hydrophobic core. In the case of $\beta = 0.25$ liposomes, our results agree well with this proposal (Fig. 8 *b*). The higher propensity toward dye-leakage in $\beta = 0.25$ liposomes in the presence of CB1 (Wang et al., 1998) may be caused by the aggregation of these peptides to form a pore (Fig. 9), which might lead to the liposome disruption. In the case of $\beta = 0.75$ liposomes, although we have also observed the insertion of the COOH-terminal α-helix of CB1 into the liposomes, as for CB1 in $\beta = 0.25$ liposomes (albeit to a less extent), the orientation of the overall peptide in the bilayer membrane may be different. Here, the lipid packing associated with a membrane containing a high concentration of PA might be tighter, and the COOH-terminal α-helix may have less tendency to insert into the bilayer membrane. In any case, we expect stronger interaction of the NH_2-terminal α-helix of CB1 with the more anionic PA lipids on the surface of $\beta = 0.75$ liposomes (Fig. 8 *a*). Both considerations would retard the insertion of the COOH-terminal α-helix into the lipid bilayer. This prediction agrees well with our earlier membrane permeability studies (Wang et al., 1998), which showed a weaker dye-leakage activity for CB1 when β is increased to 0.75 or higher.

For CB3, the interaction with the membrane is very different. Based on the observations shown in Fig. 8, *c* and *d*, only C5SL-CB3 showed sufficient binding to $\beta = 0.75$ liposomes to manifest itself. This lack of lipid binding, as revealed by studies on the spin-labeled peptides, was also noted in the spin-labeled lipid experiments (Fig. 5 *b*), and is consistent with the biosensor binding results reported recently from our laboratory (Wang et al., 1998). The association of C5SL-CB3 with lipids is apparently also different between weakly negatively charged ($\beta = 0.25$) and highly negatively charged liposomes ($\beta = 0.75$). In the former, C5SL-CB3 appears to associate with the lipids mainly through hydrophobic interactions. As the content of PA lipids is increased, electrostatic interactions involving the small number of cationic residues in CB3 may be sufficient to contribute to binding. In Fig. 7 *b*, a linear relationship is observed between bound peptide and the increase in the acidic content of the liposomes for C5SL-CB3. This observation suggests that the interaction of the NH_2-terminal region of CB3 with the lipids is enhanced by electrostatic interactions. These results support the notion that the NH_2-terminal α-helix of CB3 inserts into the lipid bilayer during the initial stages of membrane lysis. The higher membrane lysis activity of CB3 compared with CB1 on $\beta = 0.75$ liposomes observed previously (Wang et al., 1998) may therefore be interpreted in terms of the stronger binding of CB3 to the lipid surface. However, more experiments need to be performed to clarify this point.

SUMMARY

The goal of this study was to correlate the properties of the CB analogs, CB1 and CB3, which have different characteristics in their helical segments, to their ability to bind to membrane lipids and to lyse or disrupt the lipid bilayer membrane. The present investigations were carried out by ESR using both spin-labeled lipids and spin-labeled peptides. Based on the results obtained, we have developed a fairly in-depth picture on how CB1 and CB3 may bind and

interact with liposomes. To further investigate the detailed process of membrane lysis, future studies will focus on the dynamics of membrane permeabilization induced by peptides using kinetic measurements.

This work was supported in part by grant HKUST DAG97/98.SCO1 from Hong Kong University of Science and Technology (H.M.C.) and grant GM22432 from National Institutes of Health (S.I.C.).

REFERENCES

Agawa, Y., S. Lee, S. Ono, H. Aoyagi, M. Ohno, T. Taniguchi, K. Anzai, and Y. Kirino. 1991. Interaction with phospholipid bilayers, ion channel formation, and antimicrobial activity of basic amphipathic alpha-helical model peptides of various chain lengths. *J. Biol. Chem.* 266: 20218–20222.

Altenbach, C., S. L. Flitsch, H. G. Khorana, and W. L. Hubbell. 1989. Structural studies on transmembrane proteins. 2. Spin labeling of bacteriorhodopsin mutants at unique cysteines. *Biochemistry*. 28: 7806–7812.

Archer, S. J., J. F. Ellena, and D. S. Cafiso. 1991. Dynamics and aggregation of the peptide ion channel alamethicin. Measurements using spin-labeled peptides. *Biophys. J.* 60:389–398.

Barlett, G. R. 1959. Phosphorus assay in column chromatography. *J. Biol. Chem.* 234:466–468.

Ben-Tal, N., and B. Honig. 1997. Helix–helix interactions in lipid bilayers. *Biophys. J.* 71:3046–3050.

Ben-Tal, N., B. Honig, C. Miller, and S. Mclaughlin. 1997a. Electrostatic binding of proteins to membranes. Theoretical predictions and experimental results with charybdotoxin and phospholipid vesicles. *Biophys. J.* 73:1717–1727.

Ben-Tal, N., B. Honig, R. M. Peitzsch, G. Denisov, and S. McLaughlin. 1997b. Binding of small basic peptides to membranes containing acidic lipids: theoretical models and experimental results. *Biophys. J.* 71: 561–575.

Berg, S. P., and D. M. Nesbitt. 1979. Chromium oxalate: a new spin label broadening agent for use with thylakoids. *Biochim. Biophys. Acta*. 548:608–615.

Boman, H. G. 1991. Antibacterial peptides: key components needed in immunity. *Cell*. 65:205–207.

Boman, H. G. 1995. Peptide antibiotics and their role in innate immunity. *Annu. Rev. Immunol.* 13:61–92.

Castle, J. D., and W. L. Hubbell. 1976. Estimation of membrane surface potential and charge density from the phase equilibrium of a paramagnetic amphiphile. *Biochemistry*. 15:4818–4831.

Chen, H. M., W. Wang, D. Smith, and S. C. Chan. 1997. Effects of the anti-bacterial peptide cecropin B and its analogs, cecropins B-1 and B-2, on liposomes, bacteria, and cancer cells. *Biochim. Biophys. Acta*. 1336: 171–179.

Christensen, B., J. Fink, R. B. Merrifield, and D. Mauzerall. 1988. Channel-forming properties of cecropins and related model compounds incorporated into planar lipid membranes. *Proc. Natl. Acad. Sci. USA*. 85:5072–5076.

Cociancich, S., A. Ghazi, C. Hetru, J. A. Hoffmann, and L. Letellier. 1993. Insect defensin, an inducible antibacterial peptide, forms voltage-dependent channels in micrococcus luteus. *J. Biol. Chem*. 268: 19239–19245.

Cruciani, R. A., J. L. Barker, M. Zasloff, H.-C. Chen, and O. Colamonici. 1991. Antibiotic magainins exert cytolytic activity against transformed cell lines through channel formation. *Proc. Natl. Acad. Sci. USA*. 88: 3792–3796.

Dejongh, H. H., M. A. Hemminga, and D. Marsh. ESR of spin-labeled bacteriophage M13 coat protein in mixed phospholipid bilayers. 1990. *Biochim. Biophys. Acta*. 1024:82–88.

Gaffney, B. J. 1976. *In* Spin Labeling. Theory and Applications. L. J. Berliner, editor. Academic Press, New York. 567–571.

Gazit, E., A. Boman, H. G. Boman, and L. Shai. 1995. Interaction of the mammalian antibacterial peptide cecropin P1 with phospholipid vesicles. *Biochemistry*. 34:11470–11488.

Ge, M., and J. H. Freed. 1993. An electron spin resonance study of interactions between gramicidin A′ and phosphatidylcholine bilayers. *Biophys. J.* 65:2106–2123.

Holak, T. A., A. Engstrom, P. J. Kraulis, G. Lindeberg, H. Bennich, T. A. Jones, A. M. Gronenborn, and G. M. Clore. 1988. The solution conformation of the antibacterial peptide cecropin A: a nuclear magnetic resonance and dynamical simulated annealing study. *Biochemistry*. 27: 7620–7629.

Hristova, K., M. E. Selsted, and S. H. White. 1997. Critical role of lipid composition in membrane permeabilization by rabbit neutrophil defensins. *J. Biol. Chem.* 272:24224–24233.

Hultmark, D. 1993. Immune reactions in *Drosophila* and other insects: a model for innate immunity. *Trends Genet.* 9:78–183.

Hultmark, D., H. Steiner, T. Rasmuson, and H. G. Boman. 1980. Insect immunity. Purification and properties of three inducible bactericidal proteins from hemolymph of immunized pupae of *Hyalophora cecropia*. *Eur. J. Biochem.* 106:7–16.

Jaynes, J. M., G. R. Julian, G. W. Jeffers, K. L. White, and F. M. Enright. 1989. In vitro cytocidal effect of lytic peptides on several transformed mammalian cell lines. *Pept. Res.* 2:157–160.

Jost, P. C., L. J. Libertini, V. C. Hebert, and O. H. Griffith. 1971. Lipid spin labels in lecithin multilayers. A study of motion along fatty acid chains. *J. Mol. Biol.* 59:77–98.

Kagan, B. L., M. E. Selsted, T. Ganz., and R. I. Lehrer. 1990. Antimicrobial defensin peptides form voltage-dependent ion-permeable channels in planar lipid bilayer membranes. *Proc. Natl. Acad. Sci. USA*. 87: 210–214.

Keith, A., G. Bulfield, and W. Snipes. 1970. Spin-labeled *Neurospora* mitochondria. *Biophys. J.* 10:618–629.

Kim, J., M. Mosior, L. A. Chung, H. Wu, and S. McLaughlin. 1991. Binding of peptides with basic residues to membranes containing acidic phospholipids. *Biophys. J.* 60:135–148.

Kleinschmidt, J. H., J. E. Mahaney, D. D. Thomas, and D. Marsh. 1997. Interaction of bee venom melittin with zwitterionic and negatively charged phospholipid bilayers: a spin-label electron spin resonance study. *Biophys. J.* 72:767–778.

Lee, J. Y., A. Boman, C. Sun, M. Andersson, H. Jornvall, V. Mutt, and H. G. Boman. 1989. Antibacterial peptides from pig intestine: isolation of a mammalian cecropin. *Proc. Natl. Acad. Sci. USA*. 86:9159–9162.

Marsh, D., and A. Watts. 1981. Lipid-Protein Interactions. 2. P. C. Jost and O. H. Griffith, editors. John Wiley, New York.

Matsuzaki, K., A. Nakamura, O. Murase, K. Sugishita, N. Fujii, and K. Miyajima. 1997. Modulation of magainin 2-lipid bilayer interactions by peptide charge. *Biochemistry*. 36:2104–2111.

Mchaourab, H. S., J. S. Hyde, and J. B. Feix. 1993. Aggregation state of spin-labeled cecropin AD in solution. *Biochemistry*. 32:11895–11902.

Mchaourab, H. S., J. S. Hyde, and J. B. Feix. 1994. Binding and state of aggregation of spin-labeled cecropin AD in phospholipid bilayers: effects of surface charge and fatty acyl chain length. *Biochemistry*. 33: 6691–6699.

Merrifield, R. B., E. L. Merrifield, P. Juvvadi, D. Andreu, and H. G. Boman. 1994. Design and synthesis of antimicrobial peptides. *Ciba Found. Symp*. 186:5–26.

Millhauser, G. L. 1992. Selective placement of electron spin resonance spin labels: new structural methods for peptides and proteins. *TIBS*. 17:448–452.

Molin, Y. N., K. M. Salikhov, and K. I. Zamaraev. 1980. Spin Exchange. Springer-Verlag, Berlin.

Montich, G. G., C. Montecucco, E. Papini, and D. Marsh. 1995. Insertion of diphtheria toxin in lipid bilayers studied by spin label ESR. *Biochemistry*. 34:11561–11567.

Oh, K. J., H. Zhan, C. Cui, K. Hideg, R. J. Collier, and W. L. Hubbell. 1996. Organization of diphtheria toxin T domain in bilayers: a site-directed spin labeling study. *Science*. 273:810–812.

Poole, C. P. 1983. Electron Spin Resonance: A Comprehensive Treatise on Experimental Techniques. 2nd ed. Chap. 13. John Wiley and Sons, New York. 577–600.

Pouny, Y., D. Rapaport, A. Mor, P. Nicolas, and Y. Shai. 1992. Interaction of antimicrobial dermaseptin and its fluorescently labeled analogues with phospholipid membranes. *Biochemistry*. 31:12416–12423.

Saberwal, G., and R. Nagaraj. 1994. Cell-lytic and antibacterial peptides that act by perturbing the barrier function of membranes: facets of their conformational features, structure-function correlations and membrane-perturbing abilities. *Biochim. Biophys. Acta*. 1197:109–131.

Schwarz, G., S. Stankowski, and V. Rizzo. 1986. Thermodynamic analysis of incorporation and aggregation in a membrane: application to the pore-forming peptide alamethicin. *Biochim. Biophys. Acta*. 861: 141–151.

Steiner, H. 1982. Secondary structure of the cecropins: antibacterial peptides from the moth *Hyalophora cecropia. FEBS. Lett.* 137:283–287.

Steiner, H. H., D., A. Engstrom, H. Bennich, and H. G. Boman. 1981. Sequence and specificity of two antibacterial proteins involved in insect immunity. *Nature* 292:246–248.

Steiner, H., D. Andreu, and R. B. Merrifield. 1988. Binding and action of cecropin and cecropin analogues: antibacterial peptides from insects. *Biochim. Biophys. Acta*. 939:260–266.

Subczynski, W. K., and J. S. Hyde. 1981. The diffusion-concentration product of oxygen in lipid bilayers using the spin-label T1 method. *Biochim. Biophys. Acta*. 643:283–291.

Tanaka, H., and J. H. Freed. 1985. Electron spin resonance studies of lipid-gramicidin interactions utilizing oriented multibilayers. *J. Phys. Chem.* 89:350–360.

Terwilliger, T. C., and D. Eisenberg. 1982. The structure of melittin. II. Interpretation of the structure. *J. Biol. Chem.* 257:6016–6022.

Wang, W., D. K. Smith, K. Moulding, and H. M. Chen. 1998. The dependence of membrane permeability by the antibacterial peptide cecropin B and its analogs, CB-1 and CB-3, on liposomes of different composition. *J. Biol. Chem.* 273:27438–27448.

Wimley, W. C., M. E. Selsted, and S. H. White. 1994. Interactions between human defensins and lipid bilayers: evidence for formation of multimeric pores. *Protein Sci.* 3:1362–1373.

Yager, T. D., G. R. Eaton, and S. S. Eaton. 1979. Metal-nitroxyl interactions. 12. Nitroxyl spin probes in the presence of tris(oxalato) chromate(III). *Inorg. Chem.* 18:725–727.

Yin, J.-J., and Hyde, J. S. 1989. Use of high observing power in electron spin resonance saturation-recovery experiments in spin-labeled membranes. *J. Chem. Phys.* 91:6029–6035.